*DOI:*
10.1016/j.carbpol.2018.02.084

*Document Version*
Peer reviewed version

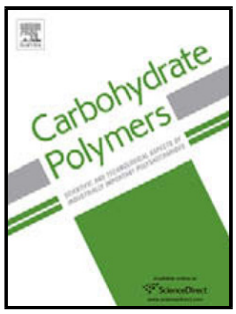


Title: Chitosan nanoparticle antigen uptake in epithelial monolayers can predict mucosal but not systemic in vivo immune response by oral delivery

Authors: Hannah Cole, Donna Bryan, Lorna Lancaster, Fatme Mawas, Driton Vllasaliu

PII: S0144-8617(18)30242-X
DOI: https://doi.org/10.1016/j.carbpol.2018.02.084
Reference: CARP 13346

To appear in:

Received date: 4-10-2017
Revised date: 6-12-2017
Accepted date: 26-2-2018

Please cite this article as: Cole, Hannah., Bryan, Donna., Lancaster, Lorna., Mawas, Fatme., & Vllasaliu, Driton., Chitosan nanoparticle antigen uptake in epithelial monolayers can predict mucosal but not systemic in vivo immune response by oral delivery.*Carbohydrate Polymers* https://doi.org/10.1016/j.carbpol.2018.02.084

# Chitosan nanoparticle antigen uptake in epithelial monolayers can predict mucosal but not systemic in vivo immune response by oral delivery

Hannah Cole[a], Donna Bryan[b], Lorna Lancaster[a], Fatme Mawas[b], Driton Vllasaliu*[a,1]

[a]School of Pharmacy, University of Lincoln, Joseph Banks Laboratories, Green Lane, Lincoln, LN6 7DL, United Kingdom

[b]Bacteriology Division, The National Institute for Biological Standards and Control (NIBSC), Blanche Lane, South Mimms, Potters Bar, EN6 3QG, United Kingdom

[1]Present address: School of Cancer and Pharmaceutical Science, 5th Floor Franklin-Wilkins Building, King's College London, 150 Stamford Street, London SE1 9NH, United Kingdom

*To whom correspondence should be addressed. Email: Driton.Vllasaliu@kcl.ac.uk, Tel: 02078481728

Hannah Cole: hannahcole27@yahoo.co.uk
Donna Bryan: Donna.Bryan@nibsc.org
Lorna Lancaster: LLancaster@lincoln.ac.uk
Fatme Mawas: Fatme.Mawas@nibsc.org
Driton Vllasaliu: Driton.Vllasaliu@kcl.ac.uk

***Highlights***

- Chitosan (CS) chloride complexes ovalbumin (OVA) model antigen into nanoparticles
- CS:OVA nanoparticles displayed favourable OVA release and no notable cytotoxicity
- CS:OVA nanoparticles markedly enhanced antigen permeability in Caco-2 monolayers
- Mucosal immune response was weak; systemic immune response not apparent in mice
- Cell monolayers antigen uptake not predictive of in vivo systemic immune response

## Abstract

This study compared in vitro and in vivo antigen delivery effects of ultrapure chitosan (CS) chloride. CS nanoparticles were formulated to incorporate ovalbumin (OVA) as a model antigen and characterised for size, charge, OVA complexation and release. The effect of CS:OVA nanoparticles on cell viability, epithelial tight junctions and transepithelial permeation of OVA was tested on Caco-2 monolayer in vitro intestinal model. The system's ability to elicit immune responses was subsequently tested in vivo. The work confirmed that CS complexes with OVA into nano-size entities. Nanocomplexes displayed favourable delivery properties, namely OVA release and no notable cytotoxicity. CS:OVA markedly enhanced antigen delivery across Caco-2 monolayers. However, the system did not elicit notable in vivo immune responses (some mucosal response was apparent) following oral delivery. The study highlights that a clear effect on antigen permeability across epithelial monolayers in vitro may predict the in vivo mucosal but not systemic immune response following oral delivery.

## Keywords

Absorption enhancement; Chitosan; Chitosan nanoparticles; Oral vaccine delivery; Ovalbumin

## Introduction

Mucosal vaccination is the most effective route to induce a local protective immune response against infections originating at mucosal surfaces (Shalaby, 1995). The oral route offers potential for convenient administration of vaccines that achieve mucosal immune response following specific targeting of antigens to the gut associated lymphoid tissue (GALT). The gastrointestinal tract, however, is an environment that presents several barriers to vaccine-mediated production of mucosal immune response. The presence of these barriers necessitates the use of appropriate delivery systems to ensure antigen protection from degradation, enhanced uptake/absorption and immune cell activation.

Chitosan (CS), a polymer derived from chitin, has become one of the most researched polymers in drug delivery due to its promising utility as an absorption enhancer. The capacity of CS to facilitate drug delivery across mucosal surfaces is attributed to its mucoadhesive properties and its ability to open the epithelial tight junctions, as structures that keep adjacent epithelial cells in close proximity with one another. A number of studies by our group (Vllasaliu et al., 2012; Vllasaliu et al., 2010; Vllasaliu, Fowler, & Stolnik, 2014) have convincingly confirmed CS's ability to promote macromolecular absorption in vitro across intestinal and airway epithelial models.

CS and its soluble derivate, N-trimethyl chitosan (TMC), in both solution or particulate forms, have demonstrated clear potential for improved oral delivery of peptide and protein drugs (Chen et al., 2008; Sandri et al., 2007; van der Merwe, Verhoef, Verheijden, Kotze, & Junginger, 2004; Vllasaliu et al., 2012). CS has also been explored widely as a component of particulate delivery systems with the potential to enable clinically effective oral administration of vaccines (Guo, Li, Lin, & Zhang, 2016; Li et al., 2017; Vera Ramirez, Sharpe, & Peppas, 2017). This is because antigen encapsulation in particles is considered to be a key strategy in overcoming the hurdles of poor antigen immunogenicity and degradation in the gastrointestinal tract (Soares, Jesus, & Borges, 2017). However, it is not entirely clear presently whether the proven absorption enhancing property of CS is useful in promoting antigen uptake and a therapeutically relevant immune response following oral delivery of antigens.

M-cells in the follicle-associated epithelium (FAE) of intestinal Peyer's patches, which actively sample the gut lumen transporting antigens to the underlying mucosal lymphoid tissue for processing and initiation of an immune response, are an obvious target in oral vaccine delivery (Slutter et al., 2009). It has been shown that nanoparticles are actively taken up by the FAE through M-cells (Beloqui, Brayden, Artursson, Preat, & des Rieux, 2017). Therefore, it has been suggested that the use of a nanoparticulate delivery system may function as a double-edged sword, increasing the uptake into epithelium and subsequently the uptake into antigen presenting cells (APCs) (Slutter et al., 2009). Whether an enhanced transepithelial permeation of macromolecules (e.g. antigens), which can be afforded by CS nanoparticles, is translated into an improved immune response in vivo is not clear.

This work set out to compare the in vitro and in vivo oral vaccine delivery effects of CS chloride (213 kDa average molecular weight) as a CS salt that has consistently shown absorption enhancing properties in vitro in our previous work (Casettari et al., 2010; Vllasaliu et al., 2012; Vllasaliu et al., 2010). CS nanoparticles were formulated via a commonly employed ionic gelation method (Vllasaliu et al., 2010), incorporating ovalbumin (OVA) as a model antigen. Nanoparticles were then characterised for size, charge and ability to incorporate and release the model antigen cargo. The effect of CS:OVA nanoparticles on cell viability, epithelial tight junctions and transepithelial permeation of the antigen was tested in Caco-2 cell monolayers as an in vitro intestinal model. The system's ability to produce immune responses was subsequently tested in vivo.

## Materials and Methods

### Materials

Different types of ovalbumins were used: fluorescein isothiocyanate (FITC)-labelled ovalbumin (OVA) (FITC-OVA, 3 moles dye/mole), purchased from Thermo Fisher Scientific (USA); non-labelled OVA, purchased from Sigma-Aldrich (UK); and endotoxin-free OVA (EndoGrade®), purchased from Cambridge Bioscience (UK). Ultrapure CS chloride of 213

kDa average molecular weight ('Protasan UP CL 213') was obtained from Novamatrix (Norway). Tripolyphosphate (TPP), Triton X-100, 2-(N-morpholino)ethanesulfonic acid (MES), paraformaldehyde and Fluoroshield with DAPI were all purchased from Sigma-Aldrich (UK). Caco-2 cells were attained from the European Collection of Cell Cultures (ECACC) and used between passages 57-88. Hank's Balanced Salt Solution (HBSS) (with sodium bicarbonate, without phenol red), phosphate buffered saline (PBS) tablets and trypsin were purchased from Sigma-Aldrich (UK). Transwell permeable inserts of 12 mm diameter and 0.4 µm pore size were obtained from Costar (USA). 3-(4,5-dimethylthiazol-2-yl)-5(3-carboxymethonyphenol)-2-(4-sulfophenyl)-2H-tetrazolium (MTS) reagent, which is commercially known as 'CellTiter 96 AQueous One Solution Cell Proliferation Assay', was obtained from Promega (USA). For the lactate dehydrogenase (LDH) assay, the 'Pierce LDH Cytotoxicity Assay Kit' (Thermo Scientific, USA) was used. Goat, anti-mouse IgG H & L (Horse Radish Peroxidase, HRP) pre-absorbed was purchased from Abcam (UK). Goat, anti-mouse IgA-HRP was obtained from Invitrogen (UK) and goat, anti-mouse IgG1-HRP was sourced from Southern Biotech (USA).

**Nanoparticle formulation and characterisation**

CS:OVA nanoparticles were prepared at different ratios. First, stock solutions of 2 mg/ml CS and 2 mg/ml OVA were prepared in $dH_2O$. As a chloride salt, the specific CS used in this work dissolved in $dH_2O$ with continuous stirring in approximately 20 minutes. Once dissolved, CS was mixed with OVA, creating a 1 mg/ml concentration (both CS and OVA, i.e. 1:1 mass ratio). TPP solution (1 mg/ml in $dH_2O$) was then added dropwise using a syringe with continuous stirring. TPP was added slowly until the solution appeared opalescent, indicating the formation of nanoparticles. Unlabelled OVA was used for nanoparticle characterisation, TEER and cytotoxicity studies, while FITC-OVA was employed in system fabrication for permeability studies.

Nanoparticles were characterised for size and surface charge. Size was characterised by nanoparticle tracking analysis (NTA) using a Nanosight LM10 HS instrument (Malvern, UK). Following formulation, CS:OVA nanoparticles were diluted in $dH_2O$ or Hank's Buffered Salt Solution (HBSS), supplemented with 2-(N-morpholino)ethanesulfonic acid (MES) buffer at 10 mM to create a pH of 6.0. The latter was done to replicate the biological solution used in cell studies.

Zeta potential measurements were carried out for nanoparticles with and without OVA, both in $dH_2O$ and HBSS to compare the effect of OVA on CS nanoparticle surface charge, as well as the effect of the biological buffer (high ionic strength) on the system's surface charge. Zeta potential was measured using a Zetasizer Nano ZS instrument (Malvern, UK).

**Antigen complexation and release form nanoparticles**

CS:OVA nanoparticles (1:1 mass ratio; 1 mg/ml) were prepared as described earlier, using FITC-OVA. Fluorescence of the resulting nanoparticle suspension was measured using a Tecan Infinite M200 Pro plate reader (Tecan Group ltd, Switzerland) using excitation and emission wavelengths of 488 nm and 520 nm, respectively. 1 ml of 1 mg/ml heparin in $dH_2O$ or $dH_2O$ (control) was applied to the CS:OVA nanoparticle suspension and the mixture was incubated for 30 minutes at room temperature. Thereafter, the mixture was processed for ultrafiltration using Vivaspin centrifugal concentrator tubes of 1,000 kDa molecular weight cut-off (MWCO), using centrifugation time and force specified by the manufacturer. Following centrifugation, the fluorescence of the filtrate was measured and compared to fluorescence values prior to filtration.

**Cell culture**

Caco-2 cells were routinely maintained in 75 $cm^2$ flasks at 37 °C, 5% $CO_2$ and 95% relative humidity. Dulbeco's Modified Eagle's Medium (DMEM) was used as the culture medium; this was supplemented with antibiotic and antimycotic solution (10,000 units of penicillin, 10 mg streptomycin and 25 µg amphotericin) and 10% v/v foetal bovine serum (FBS, European origin). Culture medium was replaced every two to three days.

For use as polarised monolayers modelling the intestinal epithelium, Caco-2 cells were initially detached from flasks using trypsin and seeded on 12-well Transwell permeable

inserts at $1x10^5$ to $2x10^5$ cells per 1.1 $cm^2$ insert. Cells were then cultured for 21 days, with regular replacement of culture medium (every two to three days).

**Cell toxicity studies**

*MTS assay.* Caco-2 cells were seeded on a clear 96-well plate and incubated for 24 hours prior to the assay. Samples were applied at different concentrations in HBSS. A 10% v/v solution of Triton X-100 in HBSS was used as a positive control and HBSS as a negative control. Samples were applied for three hours, following which the assay was conducted according to manufacturer's instructions, with absorbance measurements at 490nm using a Tecan Infinite M200 Pro plate reader.

The relative cell metabolic activity (%) was calculated using the following equation:

$$\text{Relative metabolic activity } = \frac{S-T}{H-T} \times 100$$

Where: S is the absorbance of cells incubated with tested samples; T is the absorbance of cells incubated with Triton X-100; H is the absorbance of cells incubated with HBSS.

*LDH assay.* Caco-2 cells were seeded on a clear 96-well plate and cultured for 48 hours before the assay. Samples were applied dissolved in HBSS, with 10% v/v Triton X-100 in HBSS and HBSS alone used as a positive and negative controls, respectively. Samples were applied to the cells for three hours and the assay performed following the manufacturer's instructions, with absorbance measured at 490 nm by a Tecan Infinite M200 Pro plate reader.

LDH release was calculated as a percentage relative to the controls, using the following equation:

$$\text{Relative LDH release} = \frac{S-H}{T-H} X100$$

Where: S is absorbance of the tested samples; H is absorbance of HBSS; T is absorbance of Triton X-100.

**Transepithelial electrical resistance studies**

Transepithelial electrical resistance (TEER) studies were conducted to measure the tight junction-opening effect of CS:OVA. Caco-2 cell monolayers were cultured on Transwell inserts for 21 days. Culture medium was initially replaced with HBSS and the cells placed in an incubator for 40-45 minutes to allow adjustment to the change in environment. TEER was measured before sample application ('time zero'). CS:OVA samples were then applied to the apical side of cell monolayers at different concentrations, in HBSS. TEER was subsequently recorded every 30 minutes for three hours, followed by a final 'reversibility measurement', 24 hours post-sample application (samples were removed after three hours incubation and cells incubated with the culture medium until the final TEER measurement).

**OVA permeability study**

Caco-2 monolayers displaying a minimum TEER of 900 $\Omega cm^2$ were considered suitable for the permeability studies. TEER measurements were taken before the permeability study to confirm the polarity and integrity of the cell monolayers. Culture medium was replaced with HBSS and cells incubated at 37°C/5% $CO_2$ for 40-45 minutes to acclimatise to HBSS. Test samples, consisting of CS:OVA (FITC-OVA) nanoparticles were then applied on the apical side of cell monolayers. CS:OVA translocation across the cell monolayers was determined by sampling the basolateral solution (100 µl) at regular intervals (every 30 min for 3 hours), with replacement of the sampled solutions with HBSS. CS:OVA translocation was determined by quantifying FITC-OVA through fluorescence measurements (488 nm excitation and 520 nm emission).

Permeability is expressed as the apparent permeability coefficient ($P_{app}$), which was calculated using the following equation:

$$P_{app} = \left(\frac{\Delta Q}{\Delta t}\right) \text{x} \left(\frac{1}{A \times C_o}\right)$$

$P_{app}$, apparent permeability (cm/s); $\Delta Q/\Delta t$, permeability rate (amount of FITC-OVA traversing the cell layers over time); $A$, diffusion area of the layer ($cm_2$); $C_0$, apically added FITC-OVA concentration. The experiment was conducted in triplicates.

**In vivo studies**

Female BALB/c mice (6-8 weeks old) were obtained from Charles River Ltd. All animal procedures were conducted in accordance with the Home Office (scientific procedures) Act 1986). Mice were immunised weekly on four occasions at days 0, 7, 14 and 21 by oral gavage with 200 µg of free OVA, OVA and 15 µg cholera toxin (CTX), or with CS:OVA nanoparticles in sodium bicarbonate pH 8.2 (all in 8.5% sodium bicarbonate). Mice were terminally bled on day 35. Intestinal washes were prepared by removing the small intestine and washing it with a protein degradation inhibition solution (ethylenediaminetetraacetic acid (EDTA), sodium azide, trypsin inhibitor, iodoacetic acid and phenylmethylsuphonyl fluoride (PMSF)), obtained from Sigma-Aldrich Ltd, UK.

*ELISA quantification of IgG and IgA.* Endograde OVA (endotoxin free) was diluted to 10µg/ml in carbonate buffer at pH 8.2 and transferred into 96-well plates (100 µl/well). Plates were incubated at 37 °C for 90 min and then at 4 °C overnight. OVA was then aspirated and the plates washed and subsequently blocked with the assay diluent (1% w/v bovine serum albumin (BSA), 0.3% v/v Tween 20 and 0.01M EDTA in PBS) at 37 °C for 30 min. Plates were then washed and 200 µl of immune mouse sera (diluted 1:50) added to the first column; samples were then serially diluted across the plate (for IgA determination, intestinal washes were tested for IgA antibodies at a single 1:2 dilution). Samples were incubated for 90 min at room temperature and the plate washed. Goat, anti-mouse IgG-HRP antibody (diluted 1:3000 in assay diluent) or goat, anti-mouse IgA-HRP (diluted 1:2000) were applied (100 µl/well) and the plate incubated at room temperature for 90 min. Plates were then washed and 100 µl of *o*-Phenylenediamine dihydrochloride (OPD) peroxidase substrate (Sigma-Aldrich Ltd) applied (in a dark environment) for 20 min. The reaction was then stopped with hydrochloric acid and sample absorbance measured at 492 nm.

Each sample/dilution was tested in duplicates and data are presented as mean end point titre for IgG (reciprocal of serum dilution giving optical density > mean blank+2 standard deviation) and as mean optical density for the IgA response.

**Statistical Analysis**

Statistical comparisons for nanoparticle characterisation, toxicity assays, TEER and permeability studies were performed using a Students t-test for two groups and ANOVA in multiple group comparisons. Statistical analysis for ELISA data was performed using the Mann Whitney U test. p values of <0.05 were considered statistically significant.

## Results

**Nanoparticle characterisation**

Figure 1 reveals size and surface charge data for CS:OVA nanoparticles (1:1 mass ratio) in HBSS (Figure 1A) and in $dH_2O$ (Figure 1B). The data highlight a lower mean and mode of 138.1 and 126.1 nm, respectively, in HBSS compared to $dH_2O$ (411.3 and 196.5 nm, respectively). The data also show that the nanoparticles sample is relatively monodisperse in HBSS, while in $dH_2O$ particulate species of multiple sizes are present.

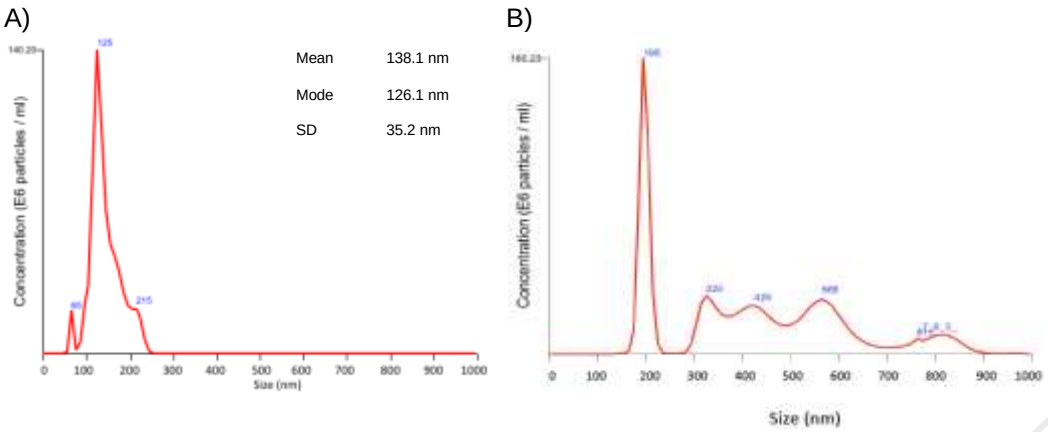


**Figure 1.** Size characterisation of CS:OVA nanoparticles in Hank's Balanced Salt Solution (HBSS) (A) and $dH_2O$ (B), using nanoparticle tracking analysis (NTA) with a Nanosight LM10 HS instrument.

Table 1 compares the zeta potential (surface charge) of CS:OVA nanoparticles against CS nanoparticles (no OVA) in HBSS and $dH_2O$. Nanoparticles displayed a lower surface charge in HBSS compared to $dH_2O$, specifically +9.68 mv and +37.9 mv, respectively. The zeta potential of CS:OVA systems (+9.68 mv) is lower compared to CS only nanoparticles (+13.1).

**Table 1.** Zeta potential comparison of CS:OVA nanoparticles against CS nanoparticles in HBSS and $dH_2O$.

| Sample | Zeta potential (mv) |
|---|---|
| CS:OVA nanoparticles in HBSS | +9.68 |
| CS nanoparticles in HBSS | +13.1 |
| CS:OVA nanoparticles in $dH_2O$ | +37.9 |
| CS nanoparticles in $dH_2O$ | +41.9 |

Complexation and release studies were carried out to determine the ability and efficiency of CS and OVA to complex into CS:OVA nanoparticles. Figure 2 shows the release of OVA from formulated CS:OVA nanoparticles (FITC-OVA was used to enable quantitation, but referred to 'OVA'). The fluorescence of 1:1 mass ratio of the systems was measured before and after FITC-OVA release, which was triggered by exposure to heparin, followed by membrane ultrafiltration (using membranes permeable to the released FITC-OVA, but not CS:OVA nanoparticles). The fluorescence intensity of CS:OVA nanoparticle filtrate not treated with heparin is dramatically lower, 499, compared to 6904 before filtration. This suggests that some, namely 6.9% OVA (calculated by converting fluorescence into amount) is lost following filtration of CS:OVA nanoparticles, most likely attributed to excess OVA unincorporated into nanoparticles. However, 93.1% of OVA remains incorporated in CS:OVA nanoparticles with 1:1 mass ratio and these did not permeate the filters due to the inability of nanoparticles to permeate membranes with 1000 kDa molecular weight cut off (MWCO). On the other hand, with samples exposed to heparin to induce OVA release and then filtered, the fluorescence intensity of the filtrate was remarkably higher compared to that of filtrate where heparin treatment was omitted. In fact, fluorescence intensity in this scenario was only slightly lower to that pre-filtration (6232.16 vs 7175), suggesting that 86.8% of OVA was released from CS:OVA nanocomplexes (and permeation through 1000 kDa MWCO ultrafiltration membranes) following exposure to heparin.

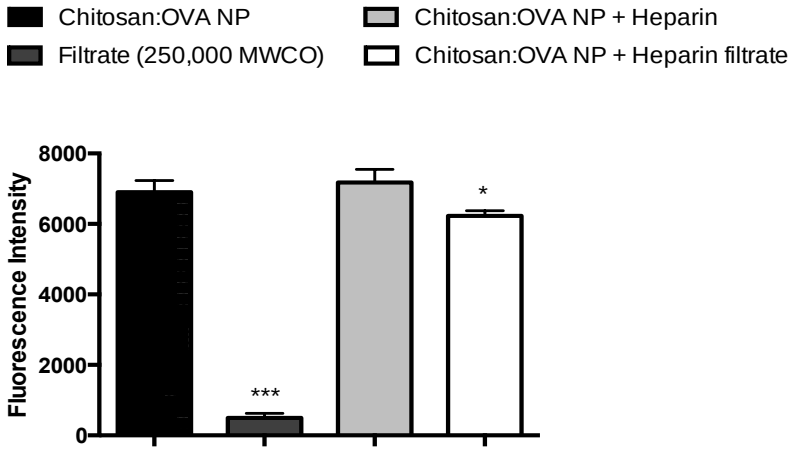


**Figure 2.** Release of FITC-OVA from chitosan:OVA nanoparticles, tested following exposure to heparin and membrane ultrafiltration. Data shown as the mean ± SD (n=3). *** signifies P=0.0002; * signifies P= 0.0356.

**Cell toxicity studies**

Figure 3A shows CS:OVA nanoparticle toxicity, as determined in Caco-2 cells via the MTS assay. The data show that the highest concentration of nanoparticles (0.1 mg/ml) resulted in a reduction of relative cell viability to approximately 62% (relative to negative control, HBSS, assumed to produce 100% viability and positive control, Triton X-100, assumed to induce total cell death and therefore 0% viability). As CS:OVA nanoparticle concentration decreased, the effect on relative cell viability diminished, although the difference between step increases in concentration was not statistically significant. CS:OVA nanoparticle concentration of 0.05 mg/ml displayed a reduction of relative cell viability to 85% and two lowest concentrations induced a small reduction of relative cell viability to 94-95%.

Membrane toxicity studies were also conducted for CS:OVA nanoparticles via the LDH assay. This assay measures the leakage of an intracellular enzyme, lactate dehydrogenase (LDH), which occurs upon plasma membrane damage. As a measure of cell membrane integrity, the LDH assay is important to study the toxicity of positively charged systems such as CS. The data in Figure 3B clearly show that CS:OVA nanoparticles were associated with low levels of LDH release (between 2-4%) in Caco-2 cells, with the difference in effect between concentrations not statistically significant.

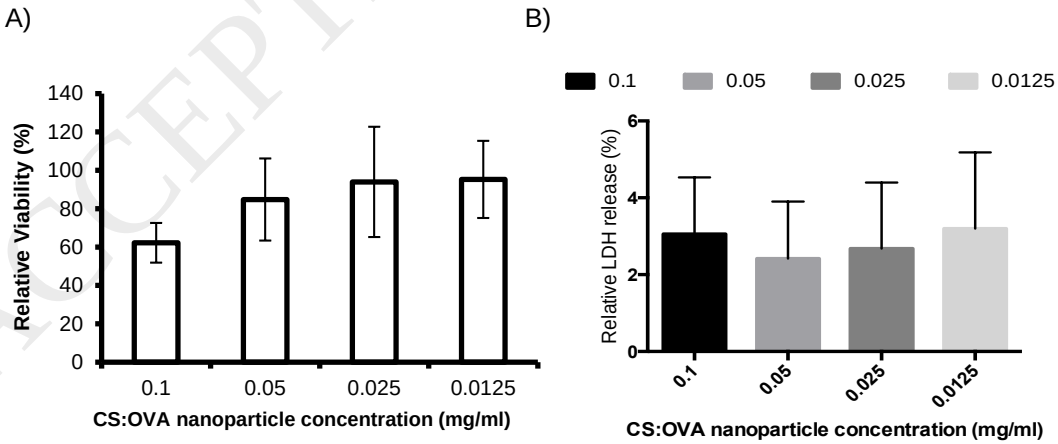


**Figure 3.** Toxicity of chitosan:ovalbumin (CS:OVA) nanoparticles. A) Effect of different concentrations of CS:OVA nanoparticles on Caco-2 relative viability, as determined by the MTS assay. Data shows the mean ± SD (n = 6). B) Effect of different concentrations of CS:OVA nanoparticles on lactate dehydrogenase (LDH) release. Hank's Balanced Salt Solution (HBSS) was used as a negative control and Triton X-100 as a positive control for cell death. Data shows the mean ± SD (n = 4).

**Transepithelial electrical resistance studies**

Figure 4 shows the effect of CS:OVA nanoparticles on Caco-2 cell monolayer TEER. Different concentrations of the systems were applied to the cells, as well as OVA itself as a control. All concentrations of CS:OVA nanoparticles caused a decrease in TEER, although application of OVA alone was in fact associated with the largest drop in TEER, by approximately 55%. However, CS:OVA nanoparticle samples caused a steeper (faster) reduction in TEER compared to OVA. In this experiment, TEER was partially reversible after 48 hours with CS:OVA samples and fully reversible with OVA.

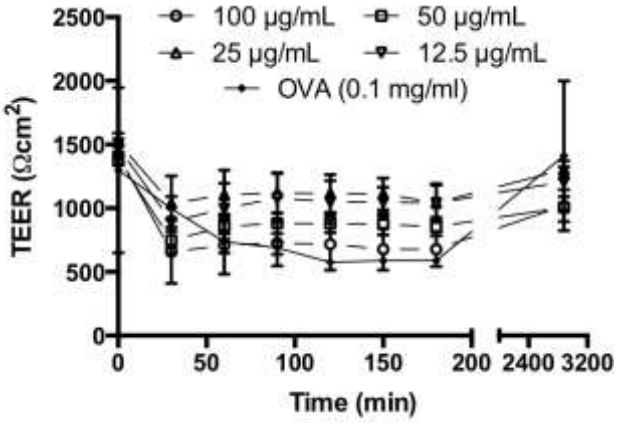


**Figure 4.** Effect of different concentrations of chitosan:ovalbumin (CS:OVA) nanoparticles and OVA at 0.1 mg/ml on Caco-2 monolayer transepithelial electrical resistance (TEER). Data shows the mean ± SD (n = 3).

**OVA permeability study**

Apical-to-basolateral permeation of FITC-OVA following application of CS:OVA nanoparticles to Caco-2 monolayers is shown in Figure 5. Note that only FITC-OVA was quantified in these studies (through fluorescence measurements) and it is not possible to state whether FITC-OVA crossed the cell monolayers complexed in CS:OVA nanoparticles or whether it was released en route. FITC-OVA permeability following application of CS:OVA nanoparticles was notably greater, specifically 4.5 times higher compared to FITC-OVA alone.

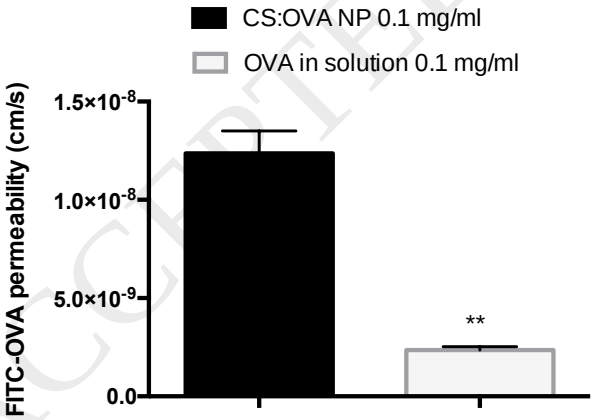


**Figure 5.** Ovalbumin (OVA) permeability following application of chitosan:ovalbumin (CS:OVA) nanoparticles at 0.1 mg/ml and comparison with OVA applied in solution (0.1 mg/ml). Fluorescently labelled ovalbumin (FITC-OVA) was used in both cases. P=0.0036. Data shows the mean ± SD (n = 3).

**In vivo studies**

The ability of CS-encapsulated OVA to induce systemic (IgG) and mucosal (IgA) immune responses following oral immunisation was evaluated by immunising mice four times at weekly intervals with CS:OVA nanoparticles, OVA alone or with OVA-CTX as controls. Data

presented in Figure 6A show that sera samples from mice immunised with OVA alone had very low level of anti-OVA IgG antibodies (mean titre = 76) and the presence of CTX as an adjuvant increased the response significantly (mean titre 922; $p<0.01$), with 3/5 mice having antibody level well above the OVA control group. However, immunisation with CS-OVA failed to increase the serum anti-OVA IgG response above the low level induced by OVA alone (mean titre = 172; $p>0.05$).

Similar to systemic IgG, free OVA induced a weak IgA response (Figure 6B) in intestinal washes (mean OD = 0.59) and mice immunised with CS:OVA had much higher level of anti-IgA response (mean OD =1.3; $p<0.01$). The increase was equal to that induced in mice immunised with OVA-CTX (mean OD = 1.3), indicating the adjuvanticity of CS for the induction of mucosal antibody response. The level of IgG and IgA response varied between low, medium and high amongst animals within the same group.

A)

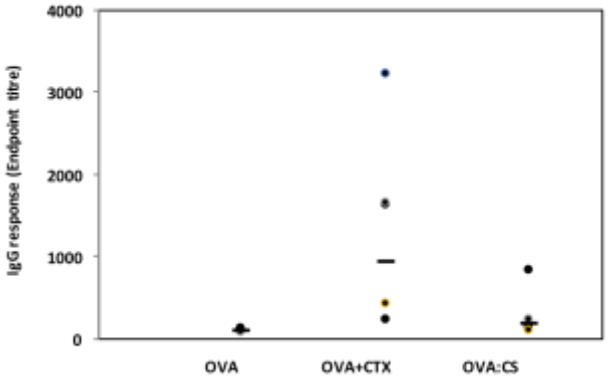


B)

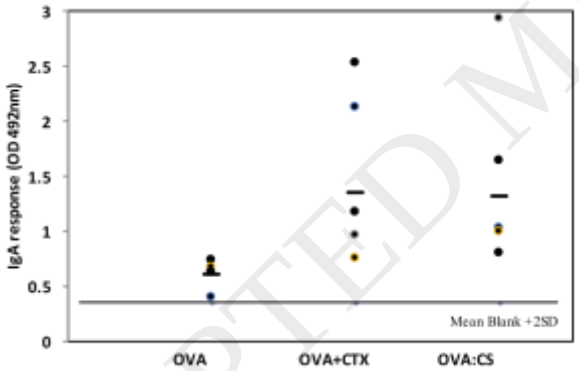


**Figure 6.** Anti-OVA antibody response following oral administration of CS:OVA nanoparticles in mice. A) Serum IgG response. B) Intestinal washes IgA response.

## Discussion

This work used a specific CS molecule (ultrapure CS chloride salt, average molecular weight 213 kDa), which has previously consistently shown substantial absorption-enhancing effects by our group, to fabricate nanocomplexes with OVA as a model antigen. The aim of the study was to establish whether macromolecular absorption enhancement, as tested in the Caco-2 in vitro intestinal epithelial monolayer model, is translated into an induction of immune response in vivo.

CS:OVA nanoparticles fabricated in this work displayed diameters below 200 nm and a positive zeta potential at 1:1 mass ratio (Figure 1 and Table 1, respectively). This is similar to previous work reporting CS:OVA nanosystems with size ranging from 83.66 nm (Wen, Xu, Zou, & Xu, 2011) to 350 nm (Amidi et al., 2006). The lower surface charge (zeta potential) of CS:OVA nanoparticles compared to CS only systems is expected due to OVA's negative charge (reported zeta potential of -20 to -25 mV (Niu et al., 2014) at pH 6.0-6.7), attenuating CS's positive surface charge. The observed zeta potential values of CS:OVA nanoparticles of 37.9 mV and 9.68 mV in $dH_2O$ and HBSS, respectively, are comparable to other studies, which reported ranges between 7.88-25 mV (Jana, Maji, Nayak, Sen, & Basu, 2013; Schrøder, Long, & Olsen, 2014).

Testing the ability of the carrier system to release the antigen payload is important as the incorporated antigen cargo must be available for immune-inducing effect. OVA release from CS:OVA nanoparticles was tested by the addition of a highly negatively charged molecule, heparin. This was based on competitive electrostatic interaction of heparin (which has a significantly higher negative charge than OVA) with the positively charged CS, releasing OVA from the nanocomplexes in the process. Following incubation with heparin and ultrafiltration, 86.8% of OVA (FITC-labelled) was released from the complexes in the filtrate, suggesting a high degree of antigen dissociation from nanocomplexes (Figure 2).

The CS:OVA nanoparticles fabricated in this work did not display appreciable toxicity to Caco-2 cells, as confirmed by MTS and LDH assays. The MTS cell viability data (Figure 3A) showed that the highest concentration of CS:OVA nanoparticles reduced Caco-2 viability between 15 and 38%, whereas the lower concentrations did not significantly reduce cell viability. The relative absence of cytotoxicity is also confirmed by the LDH assay, whereby CS:OVA nanoparticles at all tested concentrations did not significantly increase LDH release (below 5% in all cases). The relative absence of cytotoxicity with CS:OVA is likely to be helped by the presence of OVA in the system and the consequent reduction in the positive surface charge of nanoparticles, as demonstrated by zeta potential reduction. This is because charge dependency of nanoparticulate toxicity is a well demonstrated effect (Casettari et al., 2010; Naha, Davoren, Lyng, & Byrne, 2010; Schaeublin et al., 2011).

TEER experiments were conducted to ascertain whether CS:OVA nanoparticles were capable of disrupting the intestinal epithelial barrier through tight junction opening as this biological effect has been demonstrated convincingly for CS by many groups. TEER reduction was observed following sample application, although the same observation was also apparent for OVA solution at concentration equivalent to that present in nanoparticles (0.1 mg/ml). As a result, it is not clear whether CS:OVA nanoparticles exert a tight junction-modulating effect, although the pattern of TEER reduction was different with CS:OVA nanoparticles compared to OVA solution control. With all the concentrations of CS:OVA nanoparticle samples, the TEER decrease was reversible, which is another indication of non-toxicity.

CS nanoparticles have previously been shown to produce a clear effect on tight junctions, with a prior study by our group demonstrating a significant reduction of TEER (by more than 80%) in Caco-2 cell monolayers (Vllasaliu et al., 2010). It is possible that CS:OVA nanoparticles in this work did not offer a dramatic reduction in Caco-2 monolayer TEER due to surface charge reduction of the systems (from OVA presence). Such observation was reported by Sadeghi *et al.* (Sadeghi et al., 2008), showing that nanoparticles consisting of CS and its quaternary ammonium derivatives loaded with insulin were less effective in facilitating paracellular transport across Caco-2 cell monolayers compared to the corresponding free

polymers and arguing that the reduced charge density at nanoparticle surface, compared to the soluble form of CS, was responsible for this finding.

Permeability studies were performed to determine whether OVA, as a model antigen complexed with CS into nanoparticles, permeated across the intestinal epithelium (represented by the Caco-2 model). Data demonstrate that OVA permeability is 5-fold higher following application of CS:OVA compared to the equivalent concentration of OVA solution. It must be noted that due to the nature of the experimental procedure, whereby fluorescently-labelled OVA was quantified, it is not possible to establish whether CS:OVA nanoparticles permeated the cell monolayers or if OVA dissociated from the nanoparticles, before or during the transit process. The increase in OVA permeability across Caco-2 monolayers is notable considering the lack of clear effect on epithelial tight junctions. The mechanism responsible for this is therefore more likely to relate to nanoparticle uptake by, and translocation across, Caco-2 cells rather than paracellular transit. The relatively small size of CS:OVA nanoparticles prepared in this work is likely to facilitate the cell uptake of nanoparticles.

Following the demonstration of CS complexation with (and release of) OVA, a good overall toxicity profile and enhancement of OVA permeation across Caco-2 monolayers, the performance of the systems as mechanisms to promote oral vaccine delivery was evaluated in vivo. This is important as the in vitro outcome of many drug formulation systems is often not reproduced in vivo. In case of systems designed to deliver the therapeutic payload across the mucosal surfaces, current in vitro epithelial models may not faithfully represent the more complex mucosal surfaces, which consist of multiple cell types and have additional components that may act as important barriers to particulate delivery, with mucus and the basement membrane being obvious examples.

Induction of mucosal immune response following oral immunisation necessitates the use of a potent adjuvant to overcome induction of tolerance (Shalaby, W. S.1995). The immunising antigens need to reach the gut associated lymphoid tissues GALT (e.g. Peyer's patches) to be able to induce a mucosal antibody response and the draining lymph nodes and, subsequently, the primary lymphoid organs for induction of systemic immune response. It is clear from our results that oral immunisation with CS-encapsulated OVA induced a substantial mucosal IgA response, which was similar to the response induced by OVA in the presence of the potent adjuvant, CTX. Interestingly, CS:OVA failed to induce a systemic IgG response, while the co-administration of OVA and CTX was able to induce a substantial IgG response in 3 out of 5 mice. This could be attributed to the large size of the CS:OVA particles (mean 138 nm), which may be able to reach the local mucosal lymphoid tissues, but probably failed to reach the draining lymph nodes and the central lymphoid organs subsequently, which is necessary for the induction of systemic immune response. It is also possible that the immunisation regimen used does not favour induction of systemic IgG as only 3/5 animals had a good level of IgG response after OVA+CTX immunisation and further studies are needed to address this point. Interestingly, we have recently shown in our lab that induction of a substantial systemic IgG response to orally delivered antigens requires five consecutive immunisations, even in the presence of a potent adjuvant, such as CTX.

Several studies reported successful induction of systemic and mucosal antibody response following oral immunisation with CS-encapsulated antigens. For example, a study by Biswas *et al.* (Biswas, Chattopadhyay, Sen, & Saha, 2015) used BALB/b mice in oral immunisation studies using alginate-coated CS nanoparticles encapsulating measles antigen, prepared via ionotropic gelation using tripolyphosphate. The study found the presence of measles specific IgG and IgA in the serum and an increase in IgA secretion from the intestinal lavages for low molecular weight alginate-coated CS nanoparticles. Another study utilising dual tetanus and diphtheria toxoid-loaded, stable CS-glucomannan nanoassemblies demonstrated humoral, mucosal and cellular immune response by eliciting complete protective levels of anti-tetanus toxoid and anti-diphtheria toxoids antibodies (Harde, Siddhapura, Agrawal, & Jain, 2015). However, direct comparisons between this work and literature reports are not possible considering the many variables, such as different CS-based systems, incorporated antigens and immunisation regimens.

With regards to the use of in vitro models for prediction of oral vaccine delivery, the importance of reliably modelling FAE is appreciated. FAE contains both enterocytes and specialised M cells, which are key in the process of luminal sampling and transport of antigens to lymphoid tissue cells beneath, initiating the mucosal immune response (Kiyono & Fukuyama, 2004). In vitro, human M cell-like co-culture models are increasingly being used to investigate the uptake of nanoparticle-delivered antigens (des Rieux et al., 2007; Gullberg et al., 2000; Kerneis, Bogdanova, Kraehenbuhl, & Pringault, 1997; Kesisoglou, Schmiedlin-Ren, Fleisher, & Zimmermann, 2010). Although these models are labour-intensive and there is high inter-laboratory variability, partly because of different approaches used to establish filter-grown Caco-2/Raji B cell co-culture systems (Ahmad, Gogarty, Walsh, & Brayden, 2017), the use of these constructs is more appropriate in studies aiming to develop delivery systems for oral vaccine delivery. However, even in those situations one must exercise caution as these models do not represent the combination of physicochemical barriers present in the native mucosal tissue.

It is nevertheless interesting that a notably enhanced antigen permeability across the Caco-2 enterocyte system with CS:OVA nanoparticles was translated into an in vivo mucosal but not systemic immune response. This is particularly the case considering that compared with the Caco-2 monoculture used in the present study, M cell-like co-culture models are associated with increased particle translocation (Ahmad et al., 2017; Lai & D'Souza, 2008). An important conclusion from this study is that clear antigen absorption enhancement seen in vitro in the Caco-2 intestinal epithelial model, which has often been employed to study the potential of oral vaccine delivery systems, translates in mucosal but not systemic immune response following oral delivery in vivo.

## Conclusion

This work confirmed the CS's ability to complex a model antigen into nano-size entities. Although these systems show interesting effects in vitro, namely notable augmentation of antigen delivery across an intestinal epithelial monolayer model, this does not reliably predict in vivo systemic immune response following oral delivery.

## Funding

This research did not receive any specific grant from funding agencies in the public, commercial, or not-for-profit sectors.

## References

Ahmad, T., Gogarty, M., Walsh, E., & Brayden, D. J. (2017). A comparison of three Peyer's patch "M-like" cell culture models: particle uptake, bacterial interaction, and epithelial histology. *Eur J Pharm Biopharm*. doi:10.1016/j.ejpb.2017.07.013

Amidi, M., Romeijn, S. G., Borchard, G., Junginger, H. E., Hennink, W. E., & Jiskoot, W. (2006). Preparation and characterization of protein-loaded N-trimethyl chitosan nanoparticles as nasal delivery system. *J Control Release, 111*(1-2), 107-116. doi:10.1016/j.jconrel.2005.11.014

Beloqui, A., Brayden, D. J., Artursson, P., Preat, V., & des Rieux, A. (2017). A human intestinal M-cell-like model for investigating particle, antigen and microorganism translocation. *Nat Protoc, 12*(7), 1387-1399. doi:10.1038/nprot.2017.041

Biswas, S., Chattopadhyay, M., Sen, K. K., & Saha, M. K. (2015). Development and characterization of alginate coated low molecular weight chitosan nanoparticles as new carriers for oral vaccine delivery in mice. *Carbohydr Polym, 121*, 403-410. doi:10.1016/j.carbpol.2014.12.044

Casettari, L., Vllasaliu, D., Lam, J. K., Soliman, M., & Illum, L. (2012). Biomedical applications of amino acid-modified chitosans: a review. *Biomaterials, 33*(30), 7565-7583. doi:10.1016/j.biomaterials.2012.06.104

Casettari, L., Vllasaliu, D., Mantovani, G., Howdle, S. M., Stolnik, S., & Illum, L. (2010). Effect of PEGylation on the toxicity and permeability enhancement of chitosan. *Biomacromolecules, 11*(11), 2854-2865. doi:10.1021/bm100522c

Chen, F., Zhang, Z. R., Yuan, F., Qin, X., Wang, M., & Huang, Y. (2008). In vitro and in vivo study of N-trimethyl chitosan nanoparticles for oral protein delivery. *Int J Pharm, 349*(1-2), 226-233. doi:10.1016/j.ijpharm.2007.07.035

des Rieux, A., Fievez, V., Theate, I., Mast, J., Preat, V., & Schneider, Y. J. (2007). An improved in vitro model of human intestinal follicle-associated epithelium to study nanoparticle transport by M cells. *Eur J Pharm Sci, 30*(5), 380-391. doi:10.1016/j.ejps.2006.12.006

Dufes, C., Muller, J. M., Couet, W., Olivier, J. C., Uchegbu, I. F., & Schatzlein, A. G. (2004). Anticancer drug delivery with transferrin targeted polymeric chitosan vesicles. *Pharm Res, 21*(1), 101-107. doi:10.1023/B:PHAM.0000012156.65125.01

Gan, Q., & Wang, T. (2007). Chitosan nanoparticle as protein delivery carrier--systematic examination of fabrication conditions for efficient loading and release. *Colloids Surf B Biointerfaces, 59*(1), 24-34. doi:10.1016/j.colsurfb.2007.04.009

Guo, T., Li, X., Lin, M., & Zhang, L. (2016). Mucosal adjuvant activity of chitosan encapsulated nanoparticles as helicobacter pylori epitope vaccine carrier. *Nanosci Nanotechnol Lett, 8*(12), 1106-1111. doi: 10.1166/nnl.2016.2234

Gullberg, E., Leonard, M., Karlsson, J., Hopkins, A. M., Brayden, D., Baird, A. W., & Artursson, P. (2000). Expression of specific markers and particle transport in a new human intestinal M-cell model. *Biochem Biophys Res Commun, 279*(3), 808-813. doi:10.1006/bbrc.2000.4038

Harde, H., Siddhapura, K., Agrawal, A. K., & Jain, S. (2015). Divalent toxoids loaded stable chitosan-glucomannan nanoassemblies for efficient systemic, mucosal and cellular immunostimulatory response following oral administration. *Int J Pharm, 487*(1-2), 292-304. doi:10.1016/j.ijpharm.2015.04.042

Jana, S., Maji, N., Nayak, A. K., Sen, K. K., & Basu, S. K. (2013). Development of chitosan-based nanoparticles through inter-polymeric complexation for oral drug delivery. *Carbohydr Polym, 98*(1), 870-876. doi:10.1016/j.carbpol.2013.06.064

Kerneis, S., Bogdanova, A., Kraehenbuhl, J. P., & Pringault, E. (1997). Conversion by Peyer's patch lymphocytes of human enterocytes into M cells that transport bacteria. *Science, 277*(5328), 949-952. doi:10.1126/science.277.5328.949

Kesisoglou, F., Schmiedlin-Ren, P., Fleisher, D., & Zimmermann, E. M. (2010). Adenoviral transduction of enterocytes and M-cells using in vitro models based on Caco-2 cells: the coxsackievirus and adenovirus receptor (CAR) mediates both apical and basolateral transduction. *Mol Pharm, 7*(3), 619-629. doi:10.1021/mp9001377

Kiyono, H., & Fukuyama, S. (2004). NALT- versus Peyer's-patch-mediated mucosal immunity. *Nat Rev Immunol, 4*(9), 699-710. doi:10.1038/nri1439

Lai, Y. H., & D'Souza, M. J. (2008). Microparticle transport in the human intestinal M cell model. *J Drug Target, 16*(1), 36-42. doi:10.1080/10611860701639848

Li, D., Fu, D., Kang, H., Rong, G., Jin, Z, Wang, X., & Zhao, K. (2017). Advances and potential applications of chitosan nanoparticles as a delivery carrier for the mucosal immunity of vaccine. *Curr Drug Deliv*, *14*(1), 27-35. doi:10.2174/1567201813666160804121123

Naha, P. C., Davoren, M., Lyng, F. M., & Byrne, H. J. (2010). Reactive oxygen species (ROS) induced cytokine production and cytotoxicity of PAMAM dendrimers in J774A.1 cells. *Toxicol Appl Pharmacol, 246*(1-2), 91-99. doi:10.1016/j.taap.2010.04.014

Niu, F., Su, Y., Liu, Y., Wang, G., Zhang, Y., & Yang, Y. (2014). Ovalbumin-gum arabic interactions: effect of pH, temperature, salt, biopolymers ratio and total concentration. *Colloids Surf B Biointerfaces, 113*, 477-482. doi:10.1016/j.colsurfb.2013.08.012

Sadeghi, A. M., Dorkoosh, F. A., Avadi, M. R., Weinhold, M., Bayat, A., Delie, F., . . . Junginger, H. E. (2008). Permeation enhancer effect of chitosan and chitosan derivatives: comparison of formulations as soluble polymers and nanoparticulate systems on insulin absorption in Caco-2 cells. *Eur J Pharm Biopharm, 70*(1), 270-278. doi:10.1016/j.ejpb.2008.03.004

Sandri, G., Bonferoni, M. C., Rossi, S., Ferrari, F., Gibin, S., Zambito, Y., . . . Caramella, C. (2007). Nanoparticles based on N-trimethylchitosan: evaluation of absorption properties using in vitro (Caco-2 cells) and ex vivo (excised rat jejunum) models. *Eur J Pharm Biopharm, 65*(1), 68-77. doi:10.1016/j.ejpb.2006.07.016

Saranya, N., Moorthi, A., Saravanan, S., Devi, M. P., & Selvamurugan, N. (2011). Chitosan and its derivatives for gene delivery. *Int J Biol Macromol, 48*(2), 234-238. doi:10.1016/j.ijbiomac.2010.11.013

Schaeublin, N. M., Braydich-Stolle, L. K., Schrand, A. M., Miller, J. M., Hutchison, J., Schlager, J. J., & Hussain, S. M. (2011). Surface charge of gold nanoparticles mediates mechanism of toxicity. *Nanoscale, 3*(2), 410-420. doi:10.1039/c0nr00478b

Schrøder, T. D., Long, Y., & Olsen, L. F. (2014). Experimental and model study of the formation of chitosan-tripolyphosphate-siRNA nanoparticles. *Colloid and Polymer Science, 292*(11), 2869-2880. doi:10.1007/s00396-014-3331-8

Shalaby, W. S. (1995). Development of oral vaccines to stimulate mucosal and systemic immunity: barriers and novel strategies. *Clin Immunol Immunopathol, 74*(2), 127-134. doi:10.1006/clin.1995.1019

Slutter, B., Plapied, L., Fievez, V., Sande, M. A., des Rieux, A., Schneider, Y. J., . . . Preat, V. (2009). Mechanistic study of the adjuvant effect of biodegradable nanoparticles in mucosal vaccination. *J Control Release, 138*(2), 113-121. doi:10.1016/j.jconrel.2009.05.011

Soares, E., Jesus, S., & Borges, O. (2018). Oral hepatitis B vaccine: chitosan or glucan based delivery systems for efficient HBsAg immunization following subcutaneous priming. *Int J Pharm, 535*(1-2), 261-271. doi:10.1016/j.ijpharm.2017.11.009

van der Merwe, S. M., Verhoef, J. C., Verheijden, J. H., Kotze, A. F., & Junginger, H. E. (2004). Trimethylated chitosan as polymeric absorption enhancer for improved peroral delivery of peptide drugs. *Eur J Pharm Biopharm, 58*(2), 225-235. doi:10.1016/j.ejpb.2004.03.023

Vela Ramirez, J. E., Sharpe, L. A., & Peppas, N. A. (2017). Current state and challenges in developing oral vaccines. *Adv Drug Deliv Rev, 114*, 116-131. doi:10.1016/j.addr.2017.04.008

Vllasaliu, D., Casettari, L., Fowler, R., Exposito-Harris, R., Garnett, M., Illum, L., & Stolnik, S. (2012). Absorption-promoting effects of chitosan in airway and intestinal cell lines: a comparative study. *Int J Pharm, 430*(1-2), 151-160. doi:10.1016/j.ijpharm.2012.04.012

Vllasaliu, D., Exposito-Harris, R., Heras, A., Casettari, L., Garnett, M., Illum, L., & Stolnik, S. (2010). Tight junction modulation by chitosan nanoparticles: comparison with chitosan solution. *Int J Pharm, 400*(1-2), 183-193. doi:10.1016/j.ijpharm.2010.08.020

Vllasaliu, D., Fowler, R., & Stolnik, S. (2014). PEGylated nanomedicines: recent progress and remaining concerns. *Expert Opin Drug Deliv, 11*(1), 139-154. doi:10.1517/17425247.2014.866651

Wen, Z. S., Xu, Y. L., Zou, X. T., & Xu, Z. R. (2011). Chitosan nanoparticles act as an adjuvant to promote both Th1 and Th2 immune responses induced by ovalbumin in mice. *Mar Drugs, 9*(6), 1038-1055. doi:10.3390/md9061038